arXiv:1507.00437v2 [hep-ph] 25 Oct 2015

Effects of scalar mesons in a Skyrme model with hidden local symmetry

Bing-Ran He,[1, *] Yong-Liang Ma,[2, †] and Masayasu Harada[1, ‡]

[1] *Department of Physics, Nagoya University, Nagoya, 464-8602, Japan*

[2] *Center of Theoretical Physics and College of Physics, Jilin University, Changchun, 130012, China*

(Dated: October 27, 2015)

We study the effects of light scalar mesons on the skyrmion properties by constructing and examining a mesonic model including pion, rho meson, and omega meson fields as well as two-quark and four-quark scalar meson fields. In our model, the physical scalar mesons are defined as mixing states of the two- and four-quark fields. We first omit the four-quark scalar meson field from the model and find that when there is no direct coupling between the two-quark scalar meson and the vector mesons, the soliton mass is smaller and the soliton size is larger for lighter scalar mesons; when direct coupling is switched on, as the coupling strength increases, the soliton becomes heavy, and the radius of the baryon number density becomes large, as the repulsive force arising from the ω meson becomes strong. We then include the four-quark scalar meson field in the model and find that mixing between the two-quark and four-quark components of the scalar meson fields also affects the properties of the soliton. When the two-quark component of the lighter scalar meson is increased, the soliton mass decreases and the soliton size increases.

PACS numbers: 11.30.Rd, 12.39.Dc, 12.39.Fe, 14.40.Be

I. INTRODUCTION

More than 50 years ago, T. H. R. Skyrme proposed his pioneering idea that one may identify a certain nontrivial topological field configuration (soliton) in mesonic theory with the baryon [1]. Since then, this idea has been extensively applied in particle physics, nuclear physics, and also condensed matter physics [2]. The originally proposed Skyrme model include only the degree of freedom of the pion. Motivated by the essential roles of meson resonances such as the rho meson, omega meson, and light scalar mesons in nuclear physics, researchers extended the Skyrme model to Skyrme-type models to include such resonances [3, 4].

Recently, especially after the appearance of holographic models of quantum chromodynamics (QCD), the effects of some resonances on the skyrmion properties were widely explored. Some key points related to the present work are summarized as follows: (i) by dimensionally deconstructing a Yang-Mills theory in a flat four-dimensional space in the large N_c limit, it was found that as more isovector vector resonances are included, the soliton becomes lighter [5]; (ii) by using a chiral effective theory of vector mesons based on the hidden local symmetry (HLS) approach written up to the next-to-leading order, the omega meson that enters the chiral effective theory through the homogeneous Wess-Zumino term was found to provide a strong repulsive force [6, 7]; (iii) a scalar meson that is regarded as the Nambu-Goldstone boson associated with spontaneous breaking of the scale symmetry, i.e., the dilaton, was introduced to investigate its attractive effect [8–10]. It was found that the dilaton can provide an attractive force of about 100 MeV in the model, which can reproduce chiral restoration in matter.

In this paper, we explore the effect of scalar mesons made of two quarks and four quarks on the mass and size of the skyrmion by first constructing a chiral effective model including the pion, the rho meson, the omega meson, and two-quark and four-quark scalar mesons. Then, determining the parameters of the model through meson dynamics, we study the effects of the masses and constituents of the scalar mesons, as well as the strength of an interaction among the vector and scalar mesons, on the mass and size of the skyrmion.

Our findings can be summarized as follows:

1. When we switch off mixing between the two-quark and four-quark states in the model, the four-quark scalar state decouples from the model. The light scalar meson is a pure two-quark state. In such a case, we find that:
    (a) The soliton mass and size decrease with increasing mass of the light scalar meson.
    (b) The soliton mass depends on the coupling strength between the light scalar meson and the vector mesons. The result shows that the soliton mass and the size of the baryon number density increase when the coupling strength increases.
2. When we switch on mixing between the two-quark and four-quark states in the model, we find that, when the two-quark component of the lighter scalar meson is increased, the soliton mass becomes small and its size becomes large.

This paper is organized as follows. The next section describes how we construct the chiral effective model that we use in this paper and explains its typical features in relation to this work. In sec. 3, we calculate the skyrmion

---

[*] he@hken.phys.nagoya-u.ac.jp
[†] yongliangma@jlu.edu.cn
[‡] harada@hken.phys.nagoya-u.ac.jp

properties numerically and analyze the effects of scalar mesons on them. The last section discusses the results we obtained and presents our conclusions. In the appendixes, we give some details of the calculation.

II. THE MODEL

We start by constructing a chiral effective model including two-quark and four-quark scalar states. Here, we limit our discussion to the mesons, including up and down quarks. In our model, we introduce a two-quark field $M_{(2)}$ that is schematically written at the quark level as

$$\left(M_{(2)}\right)^j{}_i \sim \bar{q}_{R\,i}\, q_{L\,j} \ , \tag{1}$$

where $i, j = 1, 2$ are the flavor indices. This, at the hadron level, is rewritten in terms of the isosinglet σ field and isotriplet π fields as

$$M_{(2)} = \frac{1}{2}\left(\sigma + i\vec{\pi}\cdot\vec{\tau}\right) \ , \tag{2}$$

where $\vec{\tau}$ are the Pauli matrices. Under chiral transformation, the matrix $M_{(2)}$ transforms as

$$M_{(2)} \to g_L M_{(2)} g_R^\dagger \ , \tag{3}$$

where $g_{L,R} \in \mathrm{SU}(2)_{L,R}$. Furthermore, we can impose Z_2 symmetry as a remnant of the $\mathrm{U}(1)_A$ transformation, under which q_L and q_R transform as $q_L \to -q_L$ and $q_R \to q_R$, respectively. Therefore, the hadron field $M_{(2)}$ transforms as

$$M_{(2)} \to -M_{(2)} \ . \tag{4}$$

We introduce a four-quark field that is schematically written at the quark level as

$$\phi \ \sim \ \bar{q}_{Li}\bar{q}_{Lj}\epsilon^{ij}\, q_R^k q_R^l \epsilon_{kl} \ . \tag{5}$$

In this work, we regard ϕ as a real field by considering only the real part of Eq. (5). Under the Z_2 transformation, ϕ transforms as

$$\phi \to \phi \ . \tag{6}$$

On the basis of chiral symmetry and Z_2 symmetry, the Lagrangian is written in the form

$$\begin{aligned}\mathcal{L} = \mathrm{Tr}\left(\partial_\mu M_{(2)}\partial^\mu M_{(2)}^\dagger\right) + \frac{1}{2}\partial_\mu\phi\partial^\mu\phi \\ - \left(V_0 - \bar{V}_0\right) - \left(V_{\mathrm{SB}} - \bar{V}_{\mathrm{SB}}\right) \ ,\end{aligned} \tag{7}$$

where V_0 represents the meson potential term, and V_{SB} denotes the explicit chiral symmetry breaking term, which has values of $\bar{V}_0$ and $\bar{V}_{\mathrm{SB}}$, respectively, in vacuum. We note that, in this analysis, we include only the non-derivative interactions. We require that the number of fields in each vertex derived from the potential V_0 is less than or equal to four, and the number of quarks included in each vertex is less than or equal to eight [11]. Then, the potential is expressed as

$$\begin{aligned}V_0 = \lambda\,\mathrm{Tr}\left(M_{(2)}M_{(2)}^\dagger M_{(2)}M_{(2)}^\dagger\right) - m_2^2\,\mathrm{Tr}\left(M_{(2)}M_{(2)}^\dagger\right) + \frac{1}{2}m_4^2\phi^2 \\ + \sqrt{2}A\left(\det\left(M_{(2)}\right) + \det\left(M_{(2)}^\dagger\right)\right)\phi \, .\end{aligned} \tag{8}$$

We adopt the simplest form of the explicit chiral symmetry breaking potential V_{SB}:

$$V_{\mathrm{SB}} = -\frac{1}{2}f_\pi\,\mathrm{Tr}\left(\chi M_{(2)}^\dagger + \chi^\dagger M_{(2)}\right) \ , \tag{9}$$

where $\chi = 2B\mathcal{M}$, and B and $\mathcal{M}$ are a constant with dimension one and the quark mass matrix, respectively. In this analysis, we consider an isospin-symmetric case, that is, $\mathcal{M} = \mathrm{diag}(\bar{m}\, , \, \bar{m})$, where $\bar{m} = (m_u + m_d)/2$. We use the pion mass as an input to determine the relevant parameters, so V_{SB} is expressed as

$$V_{\mathrm{SB}} = -\frac{1}{2}f_\pi m_\pi^2\,\mathrm{Tr}\left(M_{(2)}^\dagger + M_{(2)}\right) \ . \tag{10}$$

In this paper, we introduce the rho and omega mesons based on the HLS [12, 13]. For this purpose, we take the polar decomposition of $M_{(2)}$ as $M_{(2)} = \frac{1}{2}\xi_L^\dagger\sigma\xi_R$, where ξ_L and ξ_R, in the unitary gauge of the HLS, are expressed by the pion fields as

$$\xi_R = \xi_L^\dagger = e^{i\vec{\pi}\cdot\vec{\tau}/(2f_\pi)} \ . \tag{11}$$

Then, we write the Lagrangian (7) as

$$\begin{aligned}\mathcal{L} = \frac{1}{2}\partial_\mu\sigma\partial^\mu\sigma + \sigma^2\,\mathrm{Tr}\left(\alpha_{\perp\mu}\alpha_\perp^\mu\right) + \frac{1}{2}\partial_\mu\phi\partial^\mu\phi \\ - \left(V_0 - \bar{V}_0\right) - \left(V_{\mathrm{SB}} - \bar{V}_{\mathrm{SB}}\right) + \mathcal{L}_V \ ,\end{aligned} \tag{12}$$

where

$$\alpha_{\perp\mu} = \frac{1}{2i}\left(\partial_\mu\xi_R\cdot\xi_R^\dagger - \partial_\mu\xi_L\cdot\xi_L^\dagger\right) \ , \tag{13}$$

and the newly introduced term $\mathcal{L}_V$ represents the Lagrangian for the vector meson component, which will be explicitly given later. The potentials V_0 and V_{SB} are rewritten as

$$V_0 = \frac{1}{8}\lambda\sigma^4 - \frac{1}{2}m_2^2\sigma^2 + \frac{1}{2}m_4^2\phi^2 + \frac{1}{\sqrt{2}}A\sigma^2\phi,$$

$$V_{\rm SB} = -\frac{1}{4}m_\pi^2 f_\pi \sigma \,{\rm Tr}\left(U + U^\dagger\right) , \tag{14}$$

where $U = \xi_L^\dagger \xi_R = e^{i\vec{\pi}\cdot\vec{\tau}/f_\pi}$.

The stationary conditions of the potential of the system are obtained by taking the first derivative of the potential $V = V_0 + V_{\rm SB}$ with respect to σ and ϕ:

$$\frac{\partial V}{\partial \sigma} = \frac{1}{2}\lambda\sigma^3 - m_2^2\sigma + \sqrt{2}A\sigma\phi - m_\pi^2 f_\pi , \tag{15}$$

$$\frac{\partial V}{\partial \phi} = m_4^2\phi + \frac{1}{\sqrt{2}}A\sigma^2 . \tag{16}$$

After a suitable choice of the model parameters, σ acquires its expectation value $\sigma_{\rm vac}$, which is identified as the pion decay constant. Through the interaction between the two-quark and four-quark scalar states, a nonzero A leads to a nonzero expectation value of ϕ, i.e., $\phi_{\rm vac}$. The physical scalar meson fields are obtained from the fluctuations with respect to the relevant expectation values through $\sigma = f_\pi + \tilde{\sigma}$ and $\phi = \phi_{\rm vac} + \tilde{\phi}$, where $\phi_{\rm vac} = -\frac{Af_\pi^2}{\sqrt{2}m_4^2}$, as given in Eq. (A4).

Taking the second-order derivative, one obtains the mass matrix for σ and ϕ as

$$\begin{pmatrix} m_\sigma^2 & m_{\sigma\phi}^2 \\ m_{\phi\sigma}^2 & m_\phi^2 \end{pmatrix} = \begin{pmatrix} \lambda f_\pi^2 + m_\pi^2 & \sqrt{2}Af_\pi \\ \sqrt{2}Af_\pi & m_4^2 \end{pmatrix} . \tag{17}$$

The physical states f_{500} and f_{1370} are the mixing states of σ and ϕ through the rotation

$$\begin{pmatrix} f_{500} \\ f_{1370} \end{pmatrix} = \begin{pmatrix} \cos\theta & -\sin\theta \\ \sin\theta & \cos\theta \end{pmatrix} \begin{pmatrix} \tilde{\sigma} \\ \tilde{\phi} \end{pmatrix} , \tag{18}$$

where θ is the mixing angle. In Appendix A, we show some relations among the parameters and the physical quantities that are useful for this work. From Eq. (18) one can see that when $\cos\theta \to 0$, the physical state f_{500} is dominantly a four-quark state and f_{1370} is dominantly a two-quark state, whereas when $\cos\theta \to 1$, f_{500} is almost a two-quark state, but f_{1370} is almost a four-quark state.

Now, we are in a position to specify the vector meson component of the Lagrangian. Here we use the following form:

$$\mathcal{L}_V = \mathcal{L}_{V_0} + \mathcal{L}_{\rm anom} , \tag{19}$$

where $\mathcal{L}_{V_0}$ is the Lagrangian with only intrinsic parity-even terms, whereas $\mathcal{L}_{\rm anom}$ contains the intrinsic parity-odd terms relating to the ${\rm U}(2)_L \times {\rm U}(2)_R$ chiral anomaly.

Explicitly, the intrinsic parity-even Lagrangian $\mathcal{L}_{V_0}$ is expressed as

$$\mathcal{L}_{V_0} = a_{\rm hls}(s_0\sigma^2 + (1-s_0)F^2)\,{\rm Tr}(\hat{\alpha}_{\parallel\mu}\hat{\alpha}_\parallel^\mu) - \frac{1}{2g^2}\,{\rm Tr}(V_{\mu\nu}V^{\mu\nu}) , \tag{20}$$

where $\hat{\alpha}_\parallel^\mu$ and $V_{\mu\nu}$ are defined as

$$\hat{\alpha}_{\parallel\mu} = \frac{1}{2i}\left(\partial_\mu\xi_{\rm R}\cdot\xi_{\rm R}^\dagger + \partial_\mu\xi_{\rm L}\cdot\xi_{\rm L}^\dagger\right) - V_\mu ,$$

$$V_{\mu\nu} \equiv \partial_\mu V_\nu - \partial_\nu V_\mu - i[V_\mu, V_\nu] , \tag{21}$$

with

$$V_\mu = \frac{g}{\sqrt{2}}\begin{pmatrix} \frac{1}{\sqrt{2}}\left(\rho_\mu^0 + \omega_\mu\right) & \rho_\mu^+ \\ \rho_\mu^- & -\frac{1}{\sqrt{2}}\left(\rho_\mu^0 + \omega_\mu\right) \end{pmatrix} . \tag{22}$$

Here g is the gauge coupling constant of the HLS, $a_{\rm hls}$ and s_0 are real dimensionless parameters, and F is a constant of dimension one. When σ has its vacuum expectation value (VEV), $\sigma_{\rm vac} = f_\pi$, the vector meson mass is expressed as $m_V^2 = a_{\rm hls}g^2(s_0 f_\pi^2 + (1-s_0)F^2)$, where $a_{\rm hls}g^2 s_0 f_\pi^2$ represents the mass obtained by spontaneous chiral symmetry breaking, and $a_{\rm hls}g^2(1-s_0)F^2$ is the chiral invariant mass. In this sense, s_0 accounts for the magnitude of the vector meson mass coming from spontaneous chiral symmetry breaking. In this paper, we take $F = f_\pi$, so the vector meson mass is expressed as $m_V^2 = a_{\rm hls}g^2 f_\pi^2$, which is the standard form given in the HLS [12, 13]. Note that for $\mathcal{L}_{V_0}$, the term linear in the σ field is excluded by Z_2 symmetry, and s_0 can be both positive and negative.

The intrinsic parity-odd terms of the Lagrangian $\mathcal{L}_{\rm anom}$ in Eq. (19) read [13]

$$\int d^4x \mathcal{L}_{\rm anom} = \frac{N_c}{16\pi^2}\int_{M^4}\sum_{i=1}^{3} c_i\mathcal{L}_i , \tag{23}$$

where M^4 represents the four-dimensional Minkowski space, and

$$\begin{aligned} \mathcal{L}_1 &= i\epsilon^{\mu\nu\sigma\rho}\,{\rm Tr}\left(\alpha_{L\mu}\alpha_{L\nu}\alpha_{L\sigma}\alpha_{R\rho} - \alpha_{R\mu}\alpha_{R\nu}\alpha_{R\sigma}\alpha_{L\rho}\right) , \\ \mathcal{L}_2 &= i\epsilon^{\mu\nu\sigma\rho}\,{\rm Tr}\left(\alpha_{L\mu}\alpha_{R\nu}\alpha_{L\sigma}\alpha_{R\rho}\right) , \\ \mathcal{L}_3 &= \epsilon^{\mu\nu\sigma\rho}\,{\rm Tr}\left[F_{V\mu\nu}\left(\alpha_{L\sigma}\alpha_{R\rho} - \alpha_{R\sigma}\alpha_{L\rho}\right)\right] , \end{aligned} \tag{24}$$

in terms of the 1-form and 2-form notation with $\alpha_L = \hat{\alpha}_\parallel - \alpha_\perp$, $\alpha_R = \hat{\alpha}_\parallel + \alpha_\perp$, and $F_V = dV - iV^2$. The low-energy constants c_1, c_2, and c_3, which are difficult to fix from fundamental QCD, are usually estimated phenomenologically with respect to the experimental data [13]. In this work, we focus on the effect of scalar mesons on the skyrmion properties; therefore, we choose the parameters $c_1 = -c_2 = -2/3$ and $c_3 = 0$, which provides $\omega_\mu B^\mu$ [14].

III. NUMERICAL RESULTS FOR THE SKYRMION

In this section, we make a numerical study of the effects of scalar mesons on the soliton mass and also the root-mean-square (RMS) radii of the baryon number density and energy density. In Table. I, we summarize the parameters of the model used in this paper.

A. The ansatz

To study the properties of the soliton obtained from the Lagrangian (12), we take the standard parametriza-

f_π	92.4 MeV
m_π	139.57 MeV
N_c	3
c_1+c_2	0
c_1-c_2	$-\,4/3$
c_3	0
g	5.80 ± 0.91
$a_{\rm hls}$	2.07 ± 0.33

TABLE I: Values of the model parameters.

tions for the soliton configurations. Following Refs. [1, 14], we take the ansatz for the π, ρ and ω fields as

$$U = e^{i\boldsymbol{\tau}\cdot\hat{\boldsymbol{r}}F(r)}\,, \tag{25a}$$

$$\boldsymbol{\rho} = \frac{G(r)}{gr}(\hat{\boldsymbol{r}}\times\boldsymbol{\tau})\,, \tag{25b}$$

$$\omega_\mu = W(r)\delta_{\mu 0}\,. \tag{25c}$$

We parametrize the scalar meson fields σ and ϕ as

$$\sigma = f_\pi\left(1+\bar{\sigma}(r)\right)\,, \tag{26a}$$

$$\phi = \phi_{\rm vac}\left(1+\bar{\phi}(r)\right)\,, \tag{26b}$$

where $\bar{\sigma}(r)$ and $\bar{\phi}(r)$ are dimensionless functions. Substituting Eqs. (25) and (26) into the Lagrangian (12), one obtains the equations of motion for the profile functions $F(r)$, $G(r)$, $W(r)$, $\bar{\sigma}(r)$, and $\bar{\phi}(r)$. The detailed expressions are given in Appendix B. For the solutions with the baryon number $B=1$, the wave functions $F(r)$, $G(r)$, and $W(r)$ satisfy the following boundary conditions:

$$\begin{aligned} &F(0)=\pi, && F(\infty)=0,\\ &G(0)=-2, && G(\infty)=0,\\ &W'(0)=0, && W(\infty)=0. \end{aligned} \tag{27}$$

The boundary conditions for the profile functions of the scalar mesons are determined as follows: (I) as $r\to\infty$, the VEVs of the scalar meson fields should be reproduced, so both $\bar{\sigma}(r)$ and $\bar{\phi}(r)$ must vanish, i.e.,

$$\bar{\sigma}(\infty)=0\,,\qquad \bar{\phi}(\infty)=0\,; \tag{28}$$

(II) the second-order derivatives $\bar{\sigma}''$ and $\bar{\phi}''$ should be nonsingular as $r\to0$, in view of the last term in Eqs. (B6) and (B7); equivalently,

$$\bar{\sigma}'(0)=0\,,\qquad \bar{\phi}'(0)=0\,. \tag{29}$$

To study the RMS radius of the baryon number density of the system, we specify the baryon number current by introducing the external gauge field $\mathcal{V}_\mu$ of the $U(1)$ baryon number. Then, the baryon number current is obtained by taking a functional derivative of the total Lagrangian (12) with respect to $\mathcal{V}_\mu$. After an explicit calculation, the baryon number density B_0, which is the zeroth component of the baryon number current, is expressed as

$$\begin{aligned} B_0 = -\frac{2}{3gr^2}\Big\{& f_\pi^2 g^2 r^2 a_{\rm hls} W\left[s_0\bar{\sigma}^2+2s_0\bar{\sigma}+1\right]\\ &+F'\left[\alpha_2-2G\left(-\alpha_2+\alpha_3+\alpha_2\cos F\right)+\alpha_2\cos^2F-2\alpha_2\cos F+\left(\alpha_2-\alpha_3\right)G^2\right]\\ &-2\alpha_3\sin F G'+\alpha_1\sin^2 F F'\Big\}-\frac{\sin^2 F}{2\pi^2r^2}F'\,, \end{aligned} \tag{30}$$

where α_1, α_2, and α_3 relate to c_1, c_2, and c_3, respectively, through Eq. (B2). By using the equation of motion for W in Eq. (B5), the baryon number density is simplified as

$$B_0 = \frac{1}{r^2}\frac{d}{dr}\left(\frac{4\alpha_3\sin F(\cos F-G-1)}{3g}-\frac{2r^2W'}{3g}+\frac{\sin(2F)}{8\pi^2}-\frac{F}{4\pi^2}\right)\,, \tag{31}$$

which agrees with that obtained in Ref. [15]. Note that, by combining Eqs. (31) and (27), one can show that the baryon charge is correctly normalized as $\int_0^\infty dr^3 B_0(r)=1$.

In this analyse, we take $c_1+c_2=0$, $c_1-c_2=3/4$, and $c_3=0$; therefore, Eq. (30) is reduced to

$$B_0 = -\frac{2}{3gr^2}f_\pi^2 g^2 r^2 a_{\rm hls} W\left[s_0\bar{\sigma}^2+2s_0\bar{\sigma}+1\right]\,. \tag{32}$$

In our numerical calculation, in addition to the soliton mass, we also consider the RMS radius of the baryon number density, $\langle r^2\rangle_B^{1/2}$, and the RMS radius of the energy density, $\langle r^2\rangle_E^{1/2}$, which are defined as follows:

$$\begin{aligned} \langle r^2\rangle_B^{1/2} &= \sqrt{\int_0^\infty d^3r r^2 B_0(r)}\,,\\ \langle r^2\rangle_E^{1/2} &= \sqrt{\frac{1}{M_{\rm sol}}\int_0^\infty d^3r r^2 M_{\rm sol}(r)}\,, \end{aligned} \tag{33}$$

where $M_{\rm sol}$ is the soliton mass, and $M_{\rm sol}(r)$ is the corresponding energy density given in Eq. (B1).

B. Effects of scalar mesons

Now we are in a position to show how the scalar mesons affect the skyrmion properties.

First, we consider $A = 0$. In this case, the four-quark field ϕ decouples from the other mesons. The Lagrangian (12) is reduced to

$$\begin{aligned}\mathcal{L} = {} & \frac{1}{2}\partial_\mu\sigma\partial^\mu\sigma + \sigma^2\,\mathrm{Tr}(\alpha_{\perp\mu}\alpha_\perp^\mu) \\ & - (V_\sigma - \bar{V}_\sigma) - (V_{\mathrm{SB}} - \bar{V}_{\mathrm{SB}}) + \mathcal{L}_V\,, \qquad (34)\end{aligned}$$

where $V_\sigma = \frac{1}{8}\lambda\sigma^4 - \frac{1}{2}m_2^2\sigma^2$. The parameters λ and m_2^2 are related to the masses of σ and π through

$$\begin{aligned} m_\sigma^2 &= -m_2^2 + \frac{3}{2}\lambda f_\pi^2\,, \\ m_\pi^2 &= -m_2^2 + \frac{1}{2}\lambda f_\pi^2\,. \qquad (35)\end{aligned}$$

Here we take the empirical value of m_π as an input and regard m_σ as a parameter of the model. In addition, s_0 in $\mathcal{L}_V$ is an unfixed parameter. In the following, we study the relation between these two parameters and the skyrmion properties.

a. The effects of m_σ on the skyrmion properties. We start our discussion from the standard HLS Lagrangian [13], which is obtained by taking $s_0 = 0$ in this analysis.

We show the m_σ dependence of the soliton mass m_{sol} and the radii $\sqrt{\langle r^2\rangle_B}$ and $\sqrt{\langle r^2\rangle_E}$ in Fig. 1 and the profile functions in Fig. 2. From Fig. 1 we find that, increasing m_σ, the soliton mass m_{sol} increases. This tendency can be understood from the profile function of $\bar{\sigma}$ in Fig. 2; when the σ is heavy, the magnitude of $\bar{\sigma}$ is small. Because $\bar{\sigma} < 0$, as m_σ increases, the magnitude of $\sigma = f_\pi(1+\bar{\sigma})$ becomes large; consequently, the contribution of $\sigma^2\,\mathrm{Tr}(\alpha_{\perp\mu}\alpha_\perp^\mu)$ to the skyrmion mass becomes large. Physically, for a heavy σ, the attractive force provided by the σ is small; as a result, the soliton mass is large.

In addition, Fig. 1 tells us that when m_σ is large, the radii $\sqrt{\langle r^2\rangle_E}$ and $\sqrt{\langle r^2\rangle_B}$ are small. This result can be understood from the profile functions plotted in Fig. 2; when m_σ is large, the profile for $\bar{\sigma}$ becomes narrow. Generally, the σ supplies the attractive force, whereas the ω meson supplies the repulsive force. A narrow σ needs a narrow ω to balance the attractive and repulsive forces. The shapes of σ and ω dominate the shape of the energy distribution. As a result, the narrow σ and ω make the radius $\sqrt{\langle r^2\rangle_E}$ small. As for the radius of the baryon number density, from expression Eq. (32) with $s_0 = 0$, one can easily see that a narrow W gives a small radius $\sqrt{\langle r^2\rangle_B}$. To summarize, when m_σ is large, the effective range of the attractive and repulsive forces supplied by the σ and ω, respectively, are small; i.e., the soliton size is small.

b. The effects of s_0 on the skyrmion properties. The parameter s_0 controls the chiral invariant vector meson mass. Here, we show how s_0 influences the properties of the skyrmion by taking a typical value of the scalar meson mass, $m_\sigma = 1.37$ GeV. Our numerical results are plotted in Fig. 3.

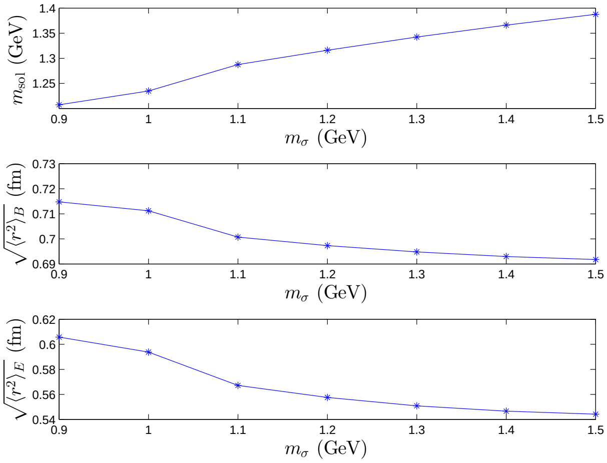

FIG. 1: m_σ dependence of the soliton mass and radii with $A = s_0 = 0$.

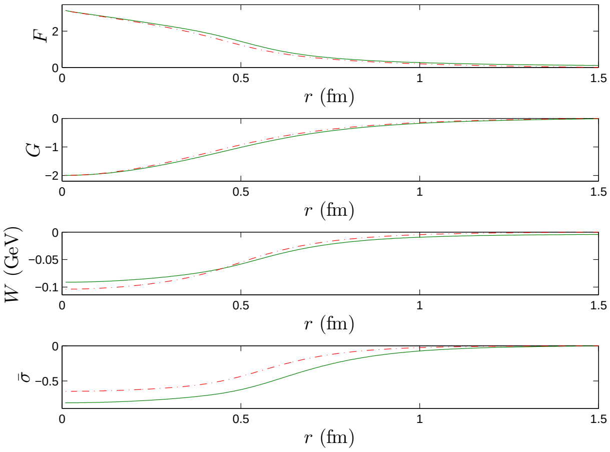

FIG. 2: m_σ dependence of the profile functions with $A = s_0 = 0$ for $m_\sigma = 1\,\mathrm{GeV}$ (green solid line) and $m_\sigma = 1.4\,\mathrm{GeV}$ (red dash-dotted line).

From Fig. 3, we see that, when the value of s_0 is increased, m_{sol} and $\sqrt{\langle r^2\rangle_B}$ become large. According to the equations of motion for the vector mesons in Eq. (B5), $a_{\mathrm{hls}}g_\omega^2\left(f_\pi^2(1-s_0) + s_0\sigma^2(r)\right)$ acts as the effective mass of the vector mesons inside the soliton. Because $\sigma(r) < f_\pi$, as we stated above, the effective mass is smaller than the meson mass $m_\omega = \sqrt{a_{\mathrm{hls}}}g_\omega f_\pi$ in vacuum. This has two effects: on the one hand, the effective strength of the repulsive force mediated by the ω meson is strong for large s_0, which produces a large soliton mass, as the vector meson dominates the energy; on the other hand, the effective range of the repulsive force supplied by ω is long for large s_0, which makes the RMS radius of the baryon number density $\sqrt{\langle r^2\rangle_B}$ large, as the ω meson acts as the gauge boson of the $U(1)_{\mathrm{V}}$ baryon number symmetry. The relation between s_0 and $\sqrt{\langle r^2\rangle_B}$ needs a more precise explanation; because the baryon number density is proportional to the effect of the ω meson, as can be seen in Eq. (32), the RMS radius of the baryon number density $\sqrt{\langle r^2\rangle_B}$ is large for large s_0.

The situation for the RMS radius of the energy density, $\sqrt{\langle r^2\rangle_E}$, is quite complicated. In this analysis, the numerical error is about 1-3%, so the third graph in Fig. 4 implies that $\sqrt{\langle r^2\rangle_E}$ is rather stable against changes in s_0. This implies that the contribution of ω has the opposite direction to that of σ, so they cancel each other.

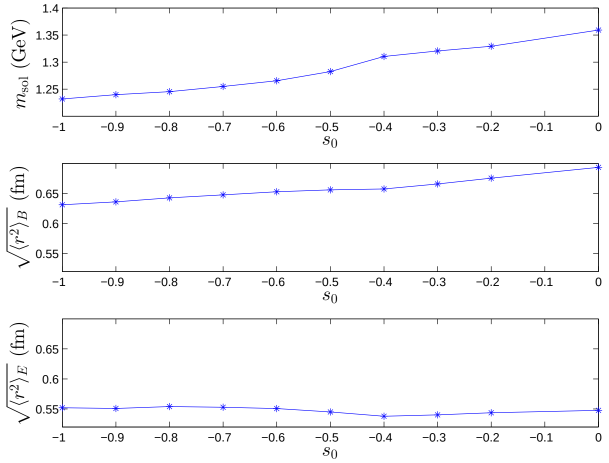

FIG. 3: s_0 dependence of the skyrmion mass and radii for $m_\sigma = 1.37$ GeV.

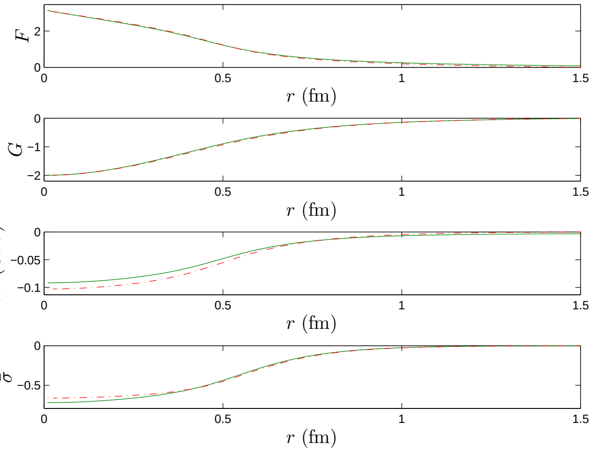

FIG. 4: Profile functions with $s_0 = -0.5$ (green line) and $s_0 = 0$ (red dotted line).

Next, we switch on the mixing between the two scalar mesons by setting $A \neq 0$ and then study how the mixing angle θ affects the skyrmion properties. In our calculation, we take two fixed values of s_0, i.e., $s_0 = 0$ and $s_0 = -0.5$, to see the dependence of the mass and radii of the skyrmion on the mixing angle θ defined in Eq. (18). Our results are shown in Figs. 5 and 6. Note that we cannot find any stable solution in the regions of $\cos\theta > 0.6$ for $s_0 = 0$ and $\cos\theta > 0.25$ for $s_0 = -0.5$. In other words, the maximal value of $\cos\theta$ is small for small s_0. This could be understood as follows. The definition of the mixing angle in Eq. (18) implies that, for a large value of $\cos\theta$, f_{500} includes a large amount of the two-quark component $\tilde{\sigma}$, which generates a strong attractive force. Because the total repulsive force does not change, the attractive force can exceed the total repulsive force, and the soliton collapses. A large value of $\cos\theta$ corresponds to a strong attractive force; therefore, the soliton collapses at a certain value of $\cos\theta$. On the other hand, a decrease in s_0 means that the repulsive force mediated by the ω meson becomes weak, as we stated above. Because the soliton is stabilized by the balance between the at-

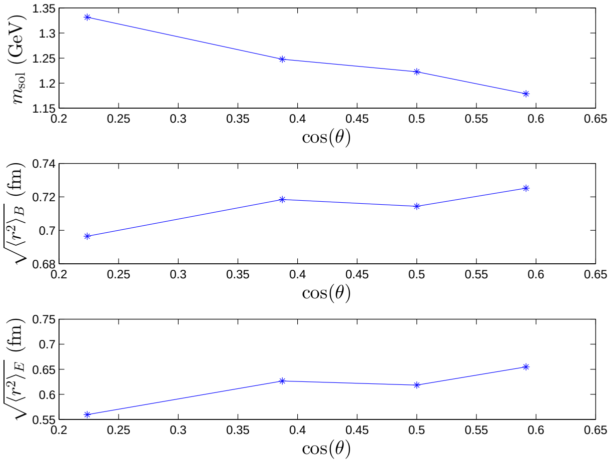

FIG. 5: Dependence of skyrmion properties on the mixing angle between two scalar mesons for $s_0 = 0$.

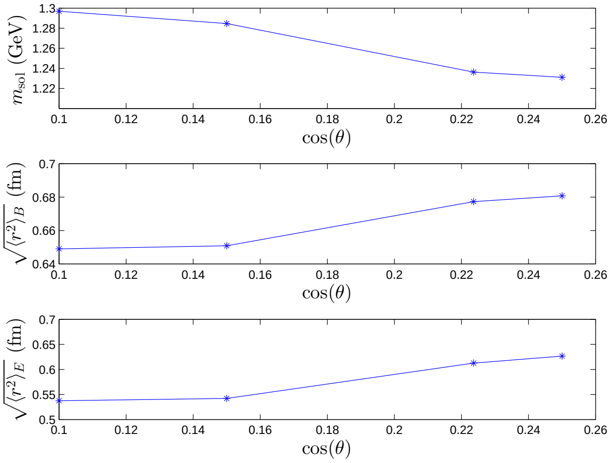

FIG. 6: Dependence of skyrmion properties on the mixing angle between two scalar mesons for $s_0 = -0.5$.

tractive and repulsive forces, the maximal value of $\cos\theta$ is small for small s_0.

Note that the decreasing and increasing tendencies in Figs. 5 and 6 are the same, and they are actually consistent with those in Fig. 1. As we just stated, increasing $\cos\theta$ increases the magnitude of the two-quark component included in f_{500}. Thus, the large $\cos\theta$ in Figs. 5 and 6 corresponds to the small mass in Fig. 1.

IV. CONCLUSIONS AND DISCUSSIONS

In this work, we first investigated the effect of a two-quark scalar meson on the skyrmion properties when mixing between the two-quark and four-quark states of scalar mesons is switched off. We found that as the mass of the two-quark scalar meson decreases, the soliton mass decreases and the RMS radii of the baryon number density, $\sqrt{\langle r^2\rangle_B}$, and the energy density, $\sqrt{\langle r^2\rangle_E}$, increase. We next studied the effect on the skyrmion properties of coupling between the scalar meson and vector mesons. It is found that as coupling becomes larger, the soliton mass and radii increase. We finally explored the skyrmion properties by considering the mixing structure of the two scalar mesons. We showed that, when the percentage of the two-quark component in the lighter scalar meson is increased, the soliton mass becomes small, and the RMS radii ($\sqrt{\langle r^2\rangle_B}$ and $\sqrt{\langle r^2\rangle_E}$) become large.

Our numerical results show that, even though the two-quark and four-quark scalar mesons are both included in the model, the soliton mass obtained here is still about 300 MeV larger than that needed to reproduce the empirical values of the nucleon mass and Δ-N mass splitting. Thus, to reproduce the baryon masses in the real world, the present model should be extended. There are several possible extensions, for example, inclusion of the effect of the dilaton as the Nambu-Goldstone boson associated with the scale symmetry breaking of QCD; the effect of the $\mathcal{O}(p^4)$ terms of the HLS, which account for the π-ρ interaction; and/or the effect of all the homogeneous Wess-Zumino terms of the HLS, which increase the number of π-ρ and/or π-ρ-ω terms. We leave these possibilities as future projects. In addition, even though the present model cannot reproduce reality, it still merits application to dense matter systems to study the effect of the scalar mesons on the phase structure of nuclear matter. We will report this progress elsewhere.

ACKNOWLEDGMENTS

M. H. was supported in part by the JSPS Grant-in-Aid for Scientific Research (S) No. 22224003 and (c) No. 24540266. And the work of Y.-L. M. was supported in part by National Science Foundation of China (NSFC) under Grant No. 11475071 and the Seeds Funding of Jilin University.

Appendix A: The mixing matrix

The masses of f_{500} and f_{1370} are

$$m_{f_{500}}^2 = \frac{1}{2}\left(- \sqrt{2f_\pi^2\left(4A^2 - \lambda m_4^2 + \lambda m_\pi^2\right) + f_\pi^4\lambda^2 + \left(m_4^2 - m_\pi^2\right)^2} + f_\pi^2\lambda + m_4^2 + m_\pi^2 \right)\,, \tag{A1}$$

$$m_{f_{1370}}^2 = \frac{1}{2}\left(\sqrt{2f_\pi^2\left(4A^2 - \lambda m_4^2 + \lambda m_\pi^2\right) + f_\pi^4\lambda^2 + \left(m_4^2 - m_\pi^2\right)^2} + f_\pi^2\lambda + m_4^2 + m_\pi^2 \right)\,. \tag{A2}$$

The mixing angle θ can be obtained as

$$\theta = \arctan\sqrt{\frac{m_{f_{1370}}^2 - m_4^2}{m_4^2 - m_{f_{500}}^2}} = \arccos\sqrt{\frac{m_4^2 - m_{f_{500}}^2}{m_{f_{1370}}^2 - m_{f_{500}}^2}}\,. \tag{A3}$$

From Eqs. (15), (16), (A1) and (A2), one gets

$$\begin{aligned} A^2 &= \frac{(m_{f_{1370}}^2 - m_4^2)(m_4^2 - m_{f_{500}}^2)}{2f_\pi^2}, \\ \lambda &= \frac{m_{f_{500}}^2 + m_{f_{1370}}^2 - m_4^2 - m_\pi^2}{f_\pi^2}, \\ \phi_{\rm vac} &= -\frac{Af_\pi^2}{\sqrt{2}m_4^2}, \\ m_2^2 &= \frac{1}{2}\left(\frac{m_{f_{500}}^2 m_{f_{1370}}^2}{m_4^2} - 3m_\pi^2\right), \end{aligned} \tag{A4}$$

with $m_{f_{500}}^2 < m_4^2 < m_{f_{1370}}^2$.

Appendix B: Soliton mass and the equations of motion for the profile functions $F(r), G(r), W(r), \bar{\sigma}(r)$ and $\bar{\phi}(r)$

Substituting the ansatz defined in Eqs. (25) and (26) to the effective Lagrangian (12), we obtain the following expression for the soliton mass:

$$\begin{aligned}
M_{\rm sol} &= 4\pi \int_0^\infty drr^2 M_{\rm sol}(r) \\
&= -4\pi \int_0^\infty dr \Big\{ \frac{1}{8} r^2 \Big\{ 4 f_\pi^2 g^2 s_0 a_{\rm hls} W^2 \bar{\sigma}(\bar{\sigma}+2) - 4 f_\pi^2 \left(\bar{\sigma}+1\right)^2 F'^2 \\
&\quad + f_\pi^2 \Big[\frac{2\left(m_4^2 - m_{f_{500}}^2\right)\left(m_{f_{1370}}^2 - m_4^2\right)\left(\bar{\sigma}+1\right)^2\left(\bar{\phi}+1\right)}{m_4^2} - \left(m_{f_{500}}^2 + m_{f_{1370}}^2 - m_4^2 - m_\pi^2\right)\left(\bar{\sigma}+1\right)^4 \\
&\quad + \frac{2\left(m_{f_{500}}^2 m_{f_{1370}}^2 - 3 m_4^2 m_\pi^2\right)\left(\bar{\sigma}+1\right)^2}{m_4^2} + \frac{\left(m_4^2 - m_{f_{500}}^2\right)\left(m_4^2 - m_{f_{1370}}^2\right)\left(\bar{\phi}+1\right)^2}{m_4^2} + 8 m_\pi^2 \left(\bar{\sigma}+1\right)\cos(F) \Big] \\
&\quad + \frac{f_\pi^2 \left(m_4^2 - m_{f_{500}}^2\right)\left(m_4^2 - m_{f_{1370}}^2\right)\bar{\phi}'^2}{m_4^4} - 4 f_\pi^2 \bar{\sigma}'^2 + 4 f_\pi^2 g^2 a_{\rm hls} W^2 - \frac{f_\pi^2 \left(m_{f_{500}}^2 m_{f_{1370}}^2 + 3 m_4^2 m_\pi^2\right)}{m_4^2} + 4 W'^2 \Big\} \\
&\quad - \frac{1}{2g^2} \Big\{ 8 f_\pi^2 g^2 a_{\rm hls} G \sin^2\left(\frac{F}{2}\right)\left(s_0 \bar{\sigma}^2 + 2 s_0 \bar{\sigma} + 1\right) - 4 f_\pi^2 g^2 \bar{\sigma}^2 \sin^2\left(\frac{F}{2}\right)\left(\left(s_0 a_{\rm hls} - 1\right)\cos(F) - s_0 a_{\rm hls} - 1\right) \\
&\quad - 8 f_\pi^2 g^2 \bar{\sigma} \sin^2\left(\frac{F}{2}\right)\left(\left(s_0 a_{\rm hls} - 1\right)\cos(F) - s_0 a_{\rm hls} - 1\right) + 2 f_\pi^2 g^2 a_{\rm hls} G^2 \left(s_0 \bar{\sigma}^2 + 2 s_0 \bar{\sigma} + 1\right) \\
&\quad + 8 f_\pi^2 g^2 a_{\rm hls} \sin^4\left(\frac{F}{2}\right) - f_\pi^2 g^2 \cos(2F) + f_\pi^2 g^2 + 2 G'^2 \Big\} \\
&\quad - \alpha_3 \left(2G\left(WF' - \sin(F) W'\right) + G^2 W F' + 2\sin(F)\left(\left(\cos(F) - 1\right) W' + W G'\right)\right) \\
&\quad + \alpha_2 W F' (-\cos(F) + G + 1)^2 + \alpha_1 W F' \sin^2(F) - \frac{G^2 (G+2)^2}{2 g^2 r^2} \Big\} ,
\end{aligned} \tag{B1}$$

with

$$\alpha_1 = \frac{3gN_c}{16\pi^2}(c_1 - c_2) \,, \alpha_2 = \frac{gN_c}{16\pi^2}(c_1 + c_2) \,, \alpha_3 = \frac{gN_c}{16\pi^2} c_3 \,. \tag{B2}$$

The equations of motion for $F(r), G(r), W(r), \bar{\sigma}(r)$ and $\bar{\phi}(r)$ are expressed as

$$\begin{aligned}
F'' &= \frac{1}{f_\pi^2 r^2 (1+\bar{\sigma})^2} \\
&\quad \times \Big\{ 2G \big(f_\pi^2 s_0 a_{\rm hls} \bar{\sigma}^2 \sin F + 2 f_\pi^2 s_0 a_{\rm hls} \bar{\sigma} \sin F + f_\pi^2 a_{\rm hls} \sin F \\
&\qquad\qquad - \alpha_2 \cos F W' - \alpha_3 \cos F W' + \alpha_2 W G' - \alpha_3 W G' + \alpha_2 W' - \alpha_3 W' \big) \\
&\qquad - f_\pi^2 \bar{\sigma} \sin F \left(4 s_0 a_{\rm hls} \cos F - 4 s_0 a_{\rm hls} - 4\cos F - r^2 m_\pi^2\right) - 2 f_\pi^2 \bar{\sigma}^2 \sin F \left(s_0 a_{\rm hls} \cos F - s_0 a_{\rm hls} - \cos F\right) \\
&\qquad - 2 f_\pi^2 r^2 F' \bar{\sigma}' - 2 f_\pi^2 r \bar{\sigma}^2 F' - 2 f_\pi^2 r \bar{\sigma} F' \left(r\bar{\sigma}' + 2\right) + 2 f_\pi^2 a_{\rm hls} \sin F - f_\pi^2 a_{\rm hls} \sin(2F) \\
&\qquad - 2 f_\pi^2 r F' + f_\pi^2 m_\pi^2 r^2 \sin F + f_\pi^2 \sin(2F) - 2\alpha_2 W \cos F G' + 2\alpha_3 W \cos F G' \\
&\qquad - \frac{1}{2}\alpha_1 \cos(2F) W' - 2\alpha_2 \cos F W' + \frac{1}{2}\alpha_2 \cos(2F) W' - 2\alpha_3 \cos F W' + 2\alpha_3 \cos(2F) W' + 2\alpha_2 W G' \\
&\qquad - 2\alpha_3 W G' + \left(\alpha_2 - \alpha_3\right) G^2 W' + \frac{1}{2}\alpha_1 W' + \frac{3}{2}\alpha_2 W' \Big\} ,
\end{aligned} \tag{B3}$$

$$\begin{aligned}
G'' = &- f_\pi^2 g^2 a_{\rm hls} \left(s_0 \bar{\sigma}^2 + 2 s_0 \bar{\sigma} + 1\right)\left(\cos F - G - 1\right) - \alpha_3 g^2 \left(W F' (\cos F - G - 1) + 2\sin F W'\right) \\
&+ \alpha_2 g^2 W F' (\cos F - G - 1) + \frac{G\left(G^2 + 3G + 2\right)}{r^2} ,
\end{aligned} \tag{B4}$$

$$\begin{aligned}
W'' &= f_\pi^2 g^2 a_{\rm hls} W \left(s_0 \bar{\sigma}^2 + 2 s_0 \bar{\sigma} + 1\right) - \frac{2W'}{r} \\
&\quad + \frac{1}{r^2} \Big\{ -\alpha_3 \left(F'\left(2G(\cos F + 1) + 2(\cos F - \cos(2F)) + G^2\right) + 4\sin F G'\right) \\
&\qquad + \alpha_2 F' (-\cos F + G + 1)^2 + 2\alpha_1 F' \sin^2\left(\frac{F}{2}\right)(\cos F + 1) \Big\} ,
\end{aligned} \tag{B5}$$

$$\begin{aligned}\bar{\sigma}'' = {}& \frac{1}{2m_4^2}\Big\{m_4^2(2\bar{\sigma}\left(-g^2 s_0 a_{\rm hls} W^2 + m_{f_{500}}^2 + m_{f_{1370}}^2 + F'^2 - m_4^2\right) + \left(m_{f_{500}}^2 + m_{f_{1370}}^2 - m_4^2 - m_\pi^2\right)\bar{\sigma}^3 \\ & + 3\left(m_{f_{500}}^2 + m_{f_{1370}}^2 - m_4^2 - m_\pi^2\right)\bar{\sigma}^2 + 2\left[-g^2 s_0 a_{\rm hls} W^2 + F'^2 - m_\pi^2(\cos F - 1)\right] \\ & - \left(m_4^2 - m_{f_{500}}^2\right)\left(m_{f_{1370}}^2 - m_4^2\right)(\bar{\sigma}+1)\,\bar{\phi}\Big\} \\ & - \frac{(\bar{\sigma}+1)\left(-8 s_0 a_{\rm hls} G \sin^2\left(\frac{F}{2}\right) - 8 s_0 a_{\rm hls}\sin^4\left(\frac{F}{2}\right) - 2 s_0 a_{\rm hls} G^2 + \cos(2F) - 1\right)}{r^2} - \frac{2\bar{\sigma}'}{r}\,, \end{aligned} \tag{B6}$$

$$\bar{\phi}'' = m_4^2\left(\bar{\phi} - \bar{\sigma}\left(\bar{\sigma}+2\right)\right) - \frac{2\bar{\phi}'}{r}\,. \tag{B7}$$

[1] T. H. R. Skyrme, Nucl. Phys. **31**, 556 (1962).

[2] For a comprehensive collection of the progress, see G.E. Brown and M. Rho, ed. *The multifaceted skyrmion* (World Scientific, Singapore 2010).

[3] For a review of early progress in this aspect, see, e.g., I. Zahed and G. E. Brown, Phys. Rept. **142**, 1 (1986).

[4] For a review, see B. -Y. Park and V. Vento, "Skyrmion approach to finite density and temperature," arXiv:0906.3263 [hep-ph], in *The Multifaceted Skyrmions* (World Scientific, Singapore, 2010) ed. G. E. Brown and M. Rho.

[5] P. Sutcliffe, JHEP **1104**, 045 (2011).

[6] Y. L. Ma, Y. Oh, G. S. Yang, M. Harada, H. K. Lee, B. Y. Park and M. Rho, Phys. Rev. D **86**, 074025 (2012) [arXiv:1206.5460 [hep-ph]].

[7] Y. L. Ma, G. S. Yang, Y. Oh and M. Harada, Phys. Rev. D **87**, no. 3, 034023 (2013) [arXiv:1209.3554 [hep-ph]].

[8] B. Y. Park, M. Rho and V. Vento, Nucl. Phys. A **736**, 129 (2004) [hep-ph/0310087].

[9] B. Y. Park, M. Rho and V. Vento, Nucl. Phys. A **807**, 28 (2008) [arXiv:0801.1374 [hep-ph]].

[10] Y. L. Ma, M. Harada, H. K. Lee, Y. Oh, B. Y. Park and M. Rho, restoration," Phys. Rev. D **90**, no. 3, 034015 (2014) [arXiv:1308.6476 [hep-ph]].

[11] A. H. Fariborz, R. Jora and J. Schechter, Phys. Rev. D **79**, 074014 (2009) [arXiv:0902.2825 [hep-ph]].

[12] M. Bando, T. Kugo and K. Yamawaki, Phys. Rept. **164**, 217 (1988).

[13] M. Harada and K. Yamawaki, Phys. Rept. **381**, 1 (2003) [hep-ph/0302103].

[14] U. G. Meissner, N. Kaiser and W. Weise, Nucl. Phys. A **466**, 685 (1987).

[15] U. G. Meissner, N. Kaiser, H. Weigel and J. Schechter, Phys. Rev. D **39**, 1956 (1989) [Erratum-ibid. D **40**, 262 (1989)].